Interaction between Caldesmon and Tropomyosin in the Presence and Absence of Smooth Muscle Actin†

Kurumi Y. Horiuchi and Samuel Chacko*
Department of Pathobiology, School of Veterinary Medicine, University of Pennsylvania, 3800 Spruce Street, Philadelphia, Pennsylvania 19104

Received April 19, 1988; Revised Manuscript Received June 23, 1988

ABSTRACT: Cysteine residues of caldesmon were labeled with the fluorescent reagent *N*-(1-pyrenyl)maleimide. The number of sulfhydryl (SH) groups in caldesmon was around 3.5 on the basis of reactivity to 5,5′-dithiobis(2-nitrobenzoate); 80% of the SH groups were labeled with pyrene. The fluorescence spectrum from pyrene-caldesmon showed the presence of excited monomer and dimer (excimer). As the ionic strength increased, excimer fluorescence decreased, disappearing at salt concentrations higher than around 50 mM. The labeling of caldesmon with pyrene did not affect its ability to inhibit actin activation of heavy meromyosin Mg–ATPase and the release of this inhibition in the presence of Ca^{2+}–calmodulin. Tropomyosin induced a change in the fluorescence spectrum of pyrene-caldesmon, indicating a conformational change associated with the interaction between caldesmon and tropomyosin. The affinity of caldesmon to tropomyosin was dependent on ionic strength. The binding constant was 5×10^6 M^{-1} in low salt, and the affinity was 20-fold less at ionic strengths close to physiological conditions. In the presence of actin, the affinity of caldesmon to tropomyosin was increased 5-fold. The addition of tropomyosin also changed the fluorescence spectrum of pyrene-caldesmon bound to actin filaments. The change in the conformation of tropomyosin, caused by the interaction between caldesmon and tropomyosin, was studied with pyrene-labeled tropomyosin. Fluorescence change was evident when unlabeled caldesmon was added to pyrene-tropomyosin bound to actin. These data suggest that the interaction between caldesmon and tropomyosin on the actin filament is associated with conformational changes on these thin filament associated proteins. These conformational changes may modulate the ability of thin filament to interact with myosin heads.

Caldesmon is an actin-binding protein that also binds to calmodulin in the presence of Ca^{2+} (Sobue et al., 1981). It is localized on thin filaments in smooth muscle and microfilaments in nonmuscle cells (Ishimura et al., 1984; Fujita et al., 1984; Bretscher & Lynch, 1985). It also causes bundling of isolated actin filaments (Sobue et al., 1982; Bretscher, 1984; Dabrowska et al., 1985). Caldesmon inhibits the actin activation of the Mg–ATPase of myosin. This inhibition is released by Ca^{2+}–calmodulin (Ngai & Walsh, 1984; Marston et al., 1985; Dabrowska et al., 1985; Sobue et al., 1985; Horiuchi et al., 1986; Lash et al., 1986; Chalovich et al., 1987). Although caldesmon binds to both actin and actin containing tropomyosin, it inhibits only the tropomyosin-enhanced Mg–ATPase of actomyosin (Sobue et al., 1985; Dabrowska et al., 1985; Marston et al., 1985; Horiuchi et al., 1986). Smooth muscle tropomyosin binds stoichiometrically to smooth muscle actin under the conditions of the ATPase assay (Miyata & Chacko, 1986). The biochemical mechanism responsible for the caldesmon-induced inhibition of tropomyosin-enhanced actomyosin ATPase is not clear. A better understanding of the interaction between the thin filament associated proteins is essential for elucidating the existence of a thin filament mediated regulation of contraction in smooth muscle.

The direct interaction between caldesmon and tropomyosin has been suggested by Graceffa (1987) on the basis of increased viscosity of tropomyosin in the presence of caldesmon in low salt and by Smith et al. (1987) on the basis of binding of tropomyosin to caldesmon–Sepharose. However, it has not been shown whether caldesmon interacts with tropomyosin bound to actin filament.

Conformational changes caused by protein–protein interaction have been studied with fluorescent probes. The fluorescent probe *N*-(1-pyrenyl)maleimide, first synthesized by Haugland (1970) and subsequently by Weltman et al. (1973), does not fluoresce in aqueous solution; however, it forms fluorescent adducts with organic compounds or proteins that contain sulfhydryl (SH)[1] groups. Pyrene covalently bound to these groups forms an excited dimer (excimer) with two adjacent SH groups. These dimers fluoresce at a wavelength longer than that at which the excited monomer fluoresces (Betcher-Lange & Lehrer, 1978). Pyrene is a useful probe in determining both SH proximity and local change in the conformation of proteins since it forms the excimer depending on the microenvironment of molecules (Graceffa & Lehrer, 1980; Ishii & Lehrer, 1985).

In this study, we labeled caldesmon with *N*-(1-pyrenyl)-maleimide and monitored fluorescence spectra to probe the conformational change of caldesmon in the presence of other thin filament associated proteins. We report that the fluorescence of pyrene-caldesmon is changed on adding tropomyosin, suggesting a direct interaction between caldesmon and tropomyosin. The tropomyosin-induced fluorescence change of pyrene-caldesmon was evident even when caldesmon was bound to smooth muscle actin prior to the addition of tropomyosin. Furthermore, when tropomyosin was labeled with pyrene and bound to actin, a change in fluorescence of pyrene-tropomyosin was observed on adding unlabeled caldesmon. These data suggest that caldesmon and tropomyosin,

† This work was supported by National Institutes of Health Grants HL 22264 and DK 39740 and NSF Grant PCM 83-09139.
* Address correspondence to this author.

[1] Abbreviations: HMM, heavy meromyosin; PMSF, phenylmethanesulfonyl fluoride; SDS, sodium dodecyl sulfate; EGTA, ethylene glycol bis(β-aminoethyl ether)-*N*,*N*,*N*′,*N*′-tetraacetic acid; EDTA, ethylenediaminetetraacetic acid; DTNB, 5,5′-dithiobis(2-nitrobenzoate); MOPS, 4-morpholinepropanesulfonic acid; SH, sulfhydryl.

0006-2960/88/0427-8388$01.50/0

located on the thin filaments, interact and that this interaction induces conformational changes in tropomyosin and caldesmon.

Materials and Methods

Gizzard actin and tropomyosin were prepared as described (Chacko, 1981; Heaslip & Chacko, 1985). Heavy meromyosin (HMM) was prepared from gizzard following the method published by Kaminski and Chacko (1984).

Gizzard caldesmon was prepared according to Bretscher (1984) with minor modifications. Gizzard was homogenized in a buffer containing 0.8 M KCl, 1 mM EGTA, 0.5 mM $MgCl_2$, 50 mM Tris-HCl (pH 7.5), 2 mM dithiothreitol, and protease inhibitors (0.5 mM PMSF, 2 μM pepstatin A, 2 μM antipain, and 0.1 mg/mL trypsin inhibitor). The residue was sedimented, and the supernatant was collected. It was subjected to further purification either without heating or after heating in a boiling water bath (90 °C, 2 min). The supernatant was then fractionated with ammonium sulfate (35–50%). The fraction was loaded into a Sepharose CL-6B column equilibrated with high-salt buffer (0.8 M KCl, 1 mM EDTA, 20 mM Tris-HCl, pH 7.5, and 1 mM dithiothreitol). The fractions containing caldesmon, determined by SDS gel electrophoresis, were purified further by chromatography on DEAE–Sephacel column (0.1–0.2 M NaCl gradient) followed by a hydroxylapatite column (0.05–0.15 M sodium phosphate gradient). Pure caldesmon was concentrated with an Amicon diaflo membrane (YM 10) and dialyzed against 50 mM KCl, 10 mM MOPS (pH 7.2), and 1 mM dithiothreitol.

Caldesmon was reduced and labeled with *N*-(1-pyrenyl)-maleimide (Polyscience) according to the method of Ishii and Lehrer (1985) except that guanidine hydrochloride was not used. After labeling, the sample was dialyzed against 50 mM KCl and 10 mM MOPS (pH 7.2). The concentration of pyrene-caldesmon was determined by the method of Lowry et al. (1951), with bovine serum albumin as a standard. The concentration of pyrene linked to caldesmon was determined from the absorbance at 343 nm with $E_{343nm} = 2.3 \times 10^4$ M^{-1} cm^{-1} (Graceffa & Lehrer, 1980). The degree of labeling was determined from the protein and the pyrene concentrations. All calculations based the molecular weight of caldesmon as 140 000. Gizzard tropomyosin was also labeled with *N*-(1-pyrenyl)maleimide as described (Lehrer et al., 1984), and the degree of labeling was 85%.

The SH content of caldesmon was determined by the method of Ellman (1959) and was calculated from A_{412nm} with $E = 13\,600$ M^{-1} cm^{-1}. The fluorescence measurements were carried out in a Perkin-Elmer 650-10S fluorescence spectrophotometer at 25 °C.

Results

Measurement of SH Group. *N*-(1-Pyrenyl)maleimide forms fluorescent adducts with sulfhydryl (SH) groups of protein (Weltman et al., 1973). The number of SH groups in the caldesmon molecule was estimated in order to determine how many pyrenes could attach to caldesmon. The SH content of caldesmon was measured with DTNB as described under Materials and Methods. Freshly made caldesmon in a solution containing dithiothreitol was passed through a G-25 column to remove dithiothreitol. In some experiments, in order to make sure that caldesmon was completely reduced, it was treated in 60 mM dithiothreitol for 1 h at 37 °C prior to passing through a G-25 column. The SH content of caldesmon was 3.5, and it was found to be the same for fresh caldesmon, reduced caldesmon, or frozen caldesmon in dithiothreitol. Frozen caldesmon, which was stored for more than 1 month, showed a decrease in the SH content, presumably due to oxidation. The heat treatment had no effect on SH composition. The color development on adding DTNB to caldesmon solution, due to the formation of SH-DTNB, was very fast, and the intensity of the color did not increase further by prolonged incubation, indicating that SH groups were completely reacted. Furthermore, the presence of urea or SDS did not make any difference in the SH content measured. These data suggest that the SH groups are located on the surface of the caldesmon molecule.

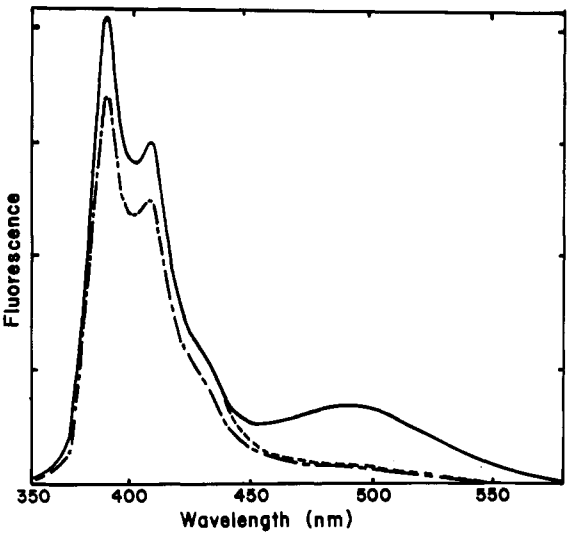

FIGURE 1: Fluorescence emission spectra of pyrene-caldesmon (0.2 μM) in 10 mM MOPS (pH 7.2) at 25 °C. The fluorescence spectra in zero KCl (—), 250 mM KCl (– – –), and 6 M urea (- - -) are shown. The excitation wavelength is at 340 nm. Monomer peaks are at 385 and 405 nm, and the excimer peak is at 490 nm.

The degree of labeling was between 2.7 and 2.9 pyrenes per mol of caldesmon, and it varied from preparation to preparation. This level of reactivity was not changed on denaturation of caldesmon by guanidine hydrochloride.

Excimer Fluorescence. The fluorescence emission spectra of pyrene-labeled caldesmon are shown in Figure 1. The monomer peaks are at 385 and 405 nm, and a broad peak at 490 nm from excimer was also observed in the low-salt condition. However, the excimer fluorescence decreased on increasing the salt concentration and was not observed above 50 mM KCl or in the presence of urea.

At high concentrations, caldesmon tends to aggregate at ionic strength lower than 50 mM. In order to rule out the possibility that excimer was caused by the interaction between pyrene groups located on different caldesmon molecules, ratios of excimer/monomer fluorescence were determined at varying concentrations of pyrene-caldesmon. The salt concentration was kept constant while the concentration of pyrene-caldesmon was increased. The excimer/monomer fluorescence ratio was not altered in the wide range of concentrations used (0.02–1.2 μM). The excimer formation did not increase on increasing the concentration of caldesmon, suggesting that the excimer was not due to aggregation of caldesmon molecules.

If caldesmon exists as a dimer as reported previously (Sobue et al., 1981; Furst et al., 1986; Cross et al., 1987), it is possible that excimer fluorescence may result from interaction between pyrenes located on the two molecules in the dimer. In order to test this possibility, pyrene-caldesmon was mixed with unlabeled caldesmon; the total caldesmon concentration was kept constant. Since the change for dimerization between pyrene-caldesmon and unlabeled caldesmon molecules was increased on mixing varied amounts of pyrene-caldesmon with unlabeled caldesmon, the ratio of excimer to monomer was

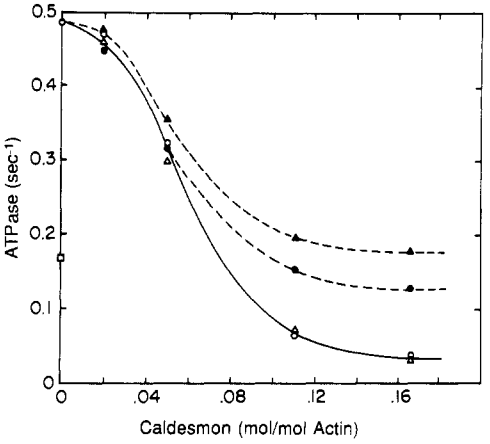

FIGURE 2: Inhibition of the actin-activated Mg–ATPase of gizzard heavy meromyosin by caldesmon. Concentrations of pyrene-caldesmon (▲, △) and unlabeled caldesmon (●, ○) vary as indicated. Conditions: 0.3 μM gizzard heavy meromyosin, 6 μM gizzard actin, 1 μM gizzard tropomyosin in 1 mM free Mg^{2+}, 2 mM Mg-ATP, 0.1 mM $CaCl_2$, 15 mM imidazole (pH 7.0), KCl to obtain an ionic strength of 0.05 M at 25 °C. Calmodulin is added to obtain a caldesmon:calmodulin molar ratio of 1:8 (●, ▲). Specific activities in the absence of caldesmon are 0.49 or 0.17 s^{-1} with (○) or without (□) tropomyosin, respectively.

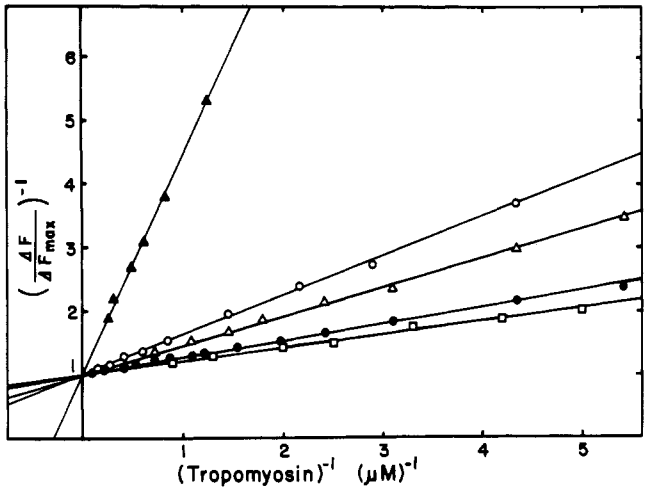

FIGURE 3: Double-inverse plots of changes in excimer fluorescence of pyrene-caldesmon as a function of the tropomyosin concentration. The concentration of pyrene-caldesmon is kept constant at 0.2 μM in 10 mM MOPS (pH 7.2) at 25 °C. Experiments are carried out either in KCl or in KCl plus $MgCl_2$. (□) 0 KCl; (●) 10 mM KCl; (○) 20 mM KCl; (△) 1 mM $MgCl_2$ + 10 mM KCl; (▲) 2 mM $MgCl_2$ + 40 mM KCl. Lines are drawn on the basis of linear least-squares regression analysis of the data. Binding constants are 5.0×10^6, 3.7×10^6, 1.7×10^6, 2.2×10^6, and 0.3×10^6 M^{-1}, respectively. Excitation wavelength, 340 nm; emission wavelength for excimer, 490 nm, and for monomer (in 2 mM $MgCl_2$ and 40 mM KCl), 405 nm.

expected to change. No change in excimer/monomer ratio was observed (data not shown). Results from this experiment indicated that excimer was formed between two SH groups on the same caldesmon molecule.

Effect of Labeling of Caldesmon with Pyrene on the Inhibition of Acto-HMM ATPase. The effect of caldesmon on the inhibition of acto-HMM ATPase was measured to determine if the functional effect of caldesmon was altered by labeling with pyrene. Unlabeled or pyrene-labeled caldesmon was added to HMM reconstituted with actin-containing tropomyosin, and the actin-activated Mg–ATPase activities were determined. As shown in Figure 2, the actin-activated Mg–ATPase activities of HMM were inhibited by both unlabeled and pyrene-labeled caldesmon. The ATP hydrolysis decreased on raising the concentration of either labeled or unlabeled caldesmon, and it leveled off at the same molar ratio of caldesmon:actin (around 1:10). This inhibition was partially released by calmodulin in both cases, although the reversibility was slightly higher when pyrene-caldesmon was used.

Effect of Tropomyosin on the Fluorescence of Pyrene-Caldesmon. Both monomer fluorescence and excimer fluorescence of pyrene-caldesmon were decreased on the addition of tropomyosin. As the change caused by tropomyosin in excimer fluorescence was higher than that in monomer fluorescence, the change in excimer fluorescence (490 nm) was monitored to determine the effect of tropomyosin on the fluorescence of pyrene-caldesmon. This experiment was done at a constant concentration of pyrene-caldesmon. The changes in excimer fluorescence versus tropomyosin concentrations plotted as the double-inverse plots are shown in Figure 3. The binding constant of caldesmon to tropomyosin, determined from the abscissa intercept of the double-inverse plot, was 5×10^6 M^{-1} at zero KCl. Constants obtained at 490 and 405 nm (monomer fluorescence) were the same. The binding constants decreased on increasing the salt concentration. Magnesium had no effect on the binding constant except for the effect due to the increase in ionic strength. At 2 mM $MgCl_2$ and 40 mM KCl, conditions used for ATPase assays (except for the absence of ATP), the binding constant was 0.3×10^6 M^{-1}. This value is 17-fold lower than that at zero KCl. Under these conditions, the change in monomer fluorescence at 405 nm was monitored, since excimer fluorescence was minimal. The affinity of caldesmon to tropomyosin became very low ($<10^5$ M^{-1}) at an ionic strength of 100 mM.

A similar experiment was done at a constant concentration of tropomyosin and increasing pyrene-caldesmon concentrations. Binding constants were the same as those of the previous experiment with increasing tropomyosin (data not shown). According to the method of Wang and Edelman (1971) to determine the stoichiometry, these results indicated that the stoichiometry of the binding of caldesmon to tropomyosin was one to one.

In order to determine if the change in fluorescence was nonspecific due to increasing the amount of protein, excimer fluorescence was measured in low salt on increasing bovine serum albumin instead of tropomyosin. The fluorescence was not changed by serum albumin (data not shown). This result suggested that the change in fluorescence by tropomyosin was not nonspecific even in low salt but rather due to an interaction between caldesmon and tropomyosin.

Interaction of Caldesmon with Tropomyosin on Actin Filament. Interaction of caldesmon to pure smooth muscle actin or actin containing bound tropomyosin was determined in 2 mM $MgCl_2$ and 40 mM KCl, since the inhibition of tropomyosin-potentiated acto-HMM ATPase was observed under this condition. Binding of pyrene-caldesmon to actin caused an increase in monomer fluorescence. Changes in fluorescence as a function of varying the concentration of pyrene-caldesmon at a constant actin concentration are depicted in Figure 4a. The change in fluorescence was saturated at an actin:caldesmon molar ratio of around 10:1. Maximal change in fluorescence was increased when tropomyosin was bound to actin, and the change was saturated at a caldesmon:tropomyosin molar ratio of 1:1 (caldesmon:actin–tropomyosin ratio of 1:7). This result suggests that an additional conformational change was induced in the caldesmon molecule by the presence of tropomyosin.

In another experiment, fluorescence change on adding tropomyosin to a constant concentration of pyrene-caldesmon that was bound to actin was measured (Figure 4b). Inter-

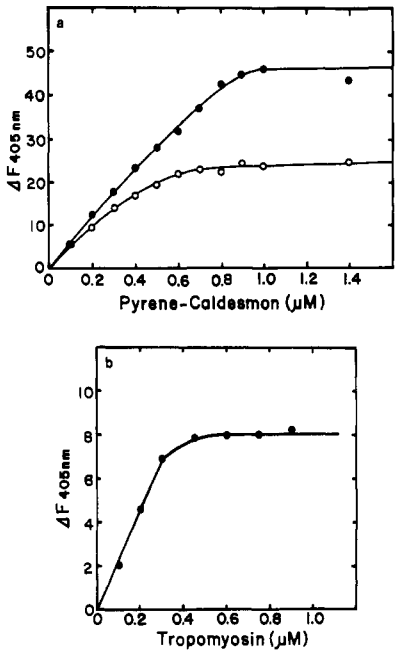

FIGURE 4: (a) Effects of F-actin or F-actin containing tropomyosin on the fluorescence of pyrene-caldesmon. The change in monomer fluorescence is monitored at 405 nm. Conditions: 6 μM actin (○) or 6 μM actin mixed with 1 μM tropomyosin (●), pyrene-caldesmon concentrations as indicated, 2 mM $MgCl_2$, 40 mM KCl, 10 mM MOPS (pH 7.2) at 25 °C. (b) Effect of tropomyosin on the fluorescence of pyrene-caldesmon bound to F-actin. Conditions are the same as in (a) except that the concentration of pyrene-caldesmon is 0.6 μM and the concentration of tropomyosin varies. Excitation wavelength, 340 nm; emission wavelength, 405 nm.

estingly, when the concentration of pyrene-caldesmon was 0.6 μM (actin:caldesmon molar ratio of 10:1), the concentration at which most caldesmon bound to actin, the fluorescence change was saturated before reaching the tropomyosin concentration, which gave a caldesmon:tropomyosin molar ratio of 1:1.

In order to confirm direct evidence for the interaction between caldesmon and tropomyosin on the actin filament, gizzard tropomyosin was labeled with pyrene as reported by Lehrer et al. (1984). Unlabeled caldesmon was added to actin containing pyrene-tropomyosin (tropomyosin:actin molar ratio of 1:6). The monomer fluorescence of pyrene-tropomyosin increased on increasing the caldesmon concentration, and the change was saturated at a caldesmon:tropomyosin molar ratio of around 1:1 (Figure 5). This result indicates that the change in fluorescence was caused by the interaction between caldesmon and the tropomyosin molecule that was bound to actin filaments.

The binding constant of caldesmon to tropomyosin bound to actin filament was calculated from Figures 4b and 5, and it was found to be 1.6×10^6 M^{-1}. This value is 5-fold higher than the binding constant (0.3×10^6 M^{-1}) obtained for caldesmon in the absence of actin (Figure 3). These data suggest strongly that the affinity of caldesmon to tropomyosin is increased in the presence of actin.

Discussion

Excimer or monomer fluorescence of *N*-(1-pyrenyl)maleimide, which covalently bound to the SH groups of cysteine in tropomyosin, has been used to determine changes in the protein conformation caused by ionic conditions and interactions between proteins (Graceffa & Lehrer, 1980; Ishii & Lehrer, 1985). In this study, we utilize this approach to investigate conformational changes on caldesmon and tropomyosin when they interact with each other on the actin filament.

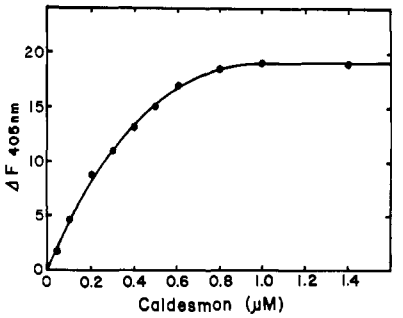

FIGURE 5: Effect of caldesmon on the fluorescence of pyrene-tropomyosin bound to F-actin. Concentrations of actin (6 μM) and pyrene-tropomyosin (1 μM) are fixed, and the concentration of unlabeled caldesmon is varied. Conditions: 2 mM $MgCl_2$, 40 mM KCl, 10 mM MOPS (pH 7.2) at 25 °C. Excitation wavelength, 340 nm; emission wavelength, 405 nm.

The number of SH groups determined in this study is 3.5. The molecular weight of caldesmon taken for this calculation is 140000, and the protein concentration is determined by the method of Lowry et al. (1951). There is a discrepancy in published reports regarding the number of cysteines in caldesmon. Ngai and Walsh (1985) report seven cysteines, and Marston et al. (1985) find no cysteine by amino acid analysis. On the other hand, Lynch et al. (1987), using a DTNB method similar to the one used in the present study, report two cysteines per caldesmon molecule. The DTNB method detects SH groups only when they are reduced; therefore, it is likely to give a cysteine value lower than the value obtained from amino acid analysis. In the study by Lynch et al. (1987), the protein concentration is determined with an extinction coefficient of $E^{1\%}_{276} = 4.9$ cm^{-1}. The protein concentration determined with this value for the extinction coefficient is lower than that determined by the method of Lowry et al. (1951). The extinction coefficient of caldesmon observed in our study is around 3.0 at 276 nm. Hence, the apparent discrepancy between the report by Lynch et al. (1987) and this study on the number of SH groups may be partly due to the difference in the method used for protein determination.

In experiments to measure the number of SH groups, the color of SH-DTNB develops immediately, and it does not require the denaturation of caldesmon. Furthermore, addition of guanidine hydrochloride during labeling does not change the amount of pyrene attached to caldesmon. Hence, unfolding of the protein structure by denaturation is not essential for SH groups of caldesmon to react with DTNB or pyrene. This indicates that the SH groups are located on the surface of the caldesmon molecule.

The presence of excimer fluorescence of pyrene covalently attached to SH groups of caldesmon indicates the proximity of two pyrenes on the same caldesmon molecule; however, it is possible that excimer is caused by aggregation of molecules. This possibility is ruled out by choosing assay conditions that prevent aggregation. Furthermore, the finding that the excimer/monomer fluorescence ratio is unchanged, when pyrene-caldesmon is mixed with unlabeled caldesmon, also shows that excimer is formed between two pyrenes attached to cysteine at close proximity in a single caldesmon molecule. The change in excimer fluorescence on raising the ionic strength is due to the lack of proximity between pyrene groups. This may be caused by a salt effect on the conformation of caldesmon molecule leading to increased rigidity.

Caldesmon inhibits the tropomyosin-enhanced actin activation of myosin ATPase, although the ATP hydrolysis con-

tinues at a level that is equivalent to that of actomyosin devoid of tropomyosin (Horiuchi et al., 1986). On the other hand, the activity of smooth muscle HMM reconstituted with actin and tropomyosin is lowered by caldesmon to a level which is below the activity of acto-HMM devoid of tropomyosin (Figure 2). This difference in the level of inhibition of the ATPase activities of actomyosin and acto-HMM by caldesmon in the presence of tropomyosin is not clear.

The ability of pyrene-labeled caldesmon to inhibit acto-HMM ATPase at the same level as the unlabeled caldesmon indicates that the functional effect, which follows the binding of caldesmon to actin, is unaffected by covalent binding of pyrene to the SH groups of caldesmon (Figure 2). The binding experiment in which caldesmon is sedimented with actin reveals that pyrene-caldesmon binds to F-actin at the same molar ratio and affinity as the unlabeled caldesmon (data not shown). The physiological significance of the conformational change associated with the interaction between caldesmon and tropomyosin is evident from the observations that pyrene-caldesmon and unlabeled caldesmon are similar in function.

Calmodulin, in the presence of Ca^{2+}, partially reverses the inhibition of the ATPase induced by both labeled and unlabeled caldesmon (Figure 2). This reversal was not increased with a higher concentration of calmodulin (data not shown). It has been shown that, at ionic strength around 50 mM (the condition used in this study), calmodulin does not reverse the inhibition caused by caldesmon completely (Horiuchi et al., 1986; Lash et al., 1986). However, the reversal in the presence of calmodulin is close to completion at ionic strengths higher than 100 mM (Smith et al., 1987). At 50 mM ionic strength, the affinity of caldesmon to actin is stronger than its affinity to calmodulin (Horiuchi & Chacko, 1988). When the ionic strength is raised from 0.05 to 0.11 M, the affinity of caldesmon to actin is decreased more than 3-fold, whereas the affinity of caldesmon to calmodulin is decreased only 1.5-fold (Horiuchi & Chacko, 1988). This difference in the ionic strength dependence for the binding of caldesmon to actin and to calmodulin may result in partial reversal of the activity by calmodulin at low ionic strength (Horiuchi et al., 1986; Lash et al., 1986) and complete reversal at ionic strength of 100 mM (Smith et al., 1987; Sobue et al., 1985).

Addition of tropomyosin to pyrene-caldesmon alters the conformation of caldesmon, as evidenced by changes in both monomer and excimer fluorescence. The binding constant between tropomyosin and caldesmon is determined from excimer fluorescence, since the change in excimer is more pronounced than the change in monomer. The binding constant decreases from 5×10^6 M^{-1} at zero KCl to 17-fold when the ionic strength is raised to 50 mM, the ionic strength used for ATPase assay. Since serum albumin fails to produce any change in pyrene-caldesmon fluorescence, the fluorescence change caused by tropomyosin is the result of a conformational change on the caldesmon molecule induced by tropomyosin. Evidence for interaction of caldesmon to tropomyosin also exists in published reports. For example, the viscosity of tropomyosin is increased on the addition of caldesmon, an indication of an interaction between caldesmon and tropomyosin (Graceffa, 1987). Interaction between caldesmon and tropomyosin has also been demonstrated by using caldesmon bound to Sepharose (Smith et al., 1987).

Caldesmon binds to tropomyosin with relatively high affinity (10^6 M^{-1} range) at low salt and low affinity ($<10^5$ M^{-1}) at ionic strength close to physiological conditions (Figure 3). In the presence of actin at 2 mM $MgCl_2$ and 40 mM KCl, caldesmon interacts to tropomyosin with a higher affinity of 1.6×10^6 M^{-1} (calculated from Figures 4b and 5) compared to the affinity in the absence of actin (0.3×10^6 M^{-1}, Figure 3). The interaction between caldesmon and tropomyosin on actin filaments, as evidenced by conformational change in our study, reveals a close proximity for these actin binding proteins on the F-actin. In the absence of actin, lowering the salt concentration may exaggerate the association between tropomyosin and caldesmon.

Caldesmon binds to isolated actin filament (Sobue et al., 1981) and native thin filament (Marston et al., 1985). The fluorescence of pyrene-caldesmon is changed when it binds to smooth muscle actin or actin–tropomyosin. These data provide evidence for a conformational change on the caldesmon molecule, associated with the interaction between thin filament associated proteins (Figure 4a,b). The presence of bound tropomyosin on the actin filament increased the fluorescence change (Figure 4a), indicating that the conformational change on caldesmon is exaggerated with tropomyosin even when it is bound to actin. This raises the possibility that the caldesmon conformation which is compatible with the inhibition of actin-activated ATPase is achieved more readily in the presence of tropomyosin.

Since caldesmon-induced inhibition of the actin-activated Mg–ATPase of smooth muscle myosin is more remarkable when the actin filament contained bound tropomyosin (Sobue et al., 1985; Horiuchi et al., 1986; Marston et al., 1985; Dabrowska et al., 1985), direct interaction between tropomyosin and caldesmon on the reconstituted thin filament observed in this study is not surprising. The change in conformation caused by protein–protein interaction is also evident when tropomyosin is labeled with pyrene and fluorescence is measured on binding of unlabeled caldesmon to actin (Figure 5). The finding that the change in fluorescence of pyrene-tropomyosin levels off at an actin:caldesmon ratio of around 10:1, a ratio close to what is needed to produce maximal inhibition of actin-activated Mg–ATPase, suggests that the conformational change on tropomyosin parallels the functional effect. This implies that the binding of caldesmon to actin, tropomyosin, or both modulates the conformation of tropomyosin on the actin filament.

In summary, results from this study indicate that the inhibitory effect of caldesmon on the activation of myosin ATPase by actin–tropomyosin is associated with conformational changes on caldesmon and tropomyosin. Furthermore, our results point out an interaction between caldesmon and tropomyosin when they are bound to actin filaments. Effects of these protein–protein interactions on the ability of thin filaments to form cross bridges with myosin filaments should be considered in future studies on the regulation of smooth muscle contraction.

ACKNOWLEDGMENTS

We are indebted to Dr. Asakura of the Children's Hospital of the University of Pennsylvania for making the fluorescence spectrophotometer available to us and to Dr. K. Horiuchi for his help with spectrofluorometry. We thank Dr. Ishii of Boston Biomedical Research Institute for valuable discussions. Gizzard used for this study was a gift from Weaver Co., New Holland, PA.

REFERENCES

Betcher-Lange, S., & Lehrer, S. S. (1978) *J. Biol. Chem. 253*, 3757–3760.

Bretscher, A. (1984) *J. Biol. Chem. 259*, 12873–12880.

Bretscher, A., & Lynch, W. (1985) *J. Cell Biol. 100*, 1656–1663.

Chacko, S. (1981) *Biochemistry 20*, 702–707.
Chalovich, J. M., Cornelius, P., & Benson, C. E. (1987) *J. Biol. Chem. 262*, 5711–5716.
Cross, R. A., Cross, K. E., & Small, J. V. (1987) *FEBS Lett. 219*, 306–310.
Dabrowska, R., Gouch, A., Galazkiewicz, B., & Osinska, H. (1985) *Biochim. Biophys. Acta 842*, 70–75.
Ellman, G. L. (1959) *Arch. Biochem. Biophys. 82*, 70–77.
Fujita, H., Ishimura, K., Ban, T., Kurosumi, M., Sobue, K., & Kakiuchi, S. (1984) *Cell Tissue Res. 237*, 375–377.
Furst, D. O., Cross, R. A., Mey, J. D., & Small, J. V. (1986) *EMBO J. 5*, 251–257.
Graceffa, P. (1987) *FEBS Lett. 218*, 139–142.
Graceffa, P., & Lehrer, S. S. (1980) *J. Biol. Chem. 255*, 11296–11300.
Haugland, R. P. (1970) Ph.D. Thesis, Stanford University, Palo Alto, CA.
Heaslip, R. J., & Chacko, S. (1985) *Biochemistry 24*, 2731–2736.
Horiuchi, K. Y., & Chacko, S. (1988) *Biophys. J. 53*, 463a.
Horiuchi, K. Y., Miyata, H., & Chacko, S. (1986) *Biochem. Biophys. Res. Commun. 136*, 962–968.
Ishii, Y., & Lehrer, S. S. (1985) *Biochemistry 24*, 6631–6638.
Ishimura, K., Fujita, H., Ban, T., Matsuda, H., Sobue, K., & Kakiuchi, S. (1984) *Cell Tissue Res. 235*, 207–209.
Kaminski, E. A., & Chacko, S. (1984) *J. Biol. Chem. 259*, 9104–9108.
Lash, J. A., Sellers, J. R., & Hathaway, D. R. (1986) *J. Biol. Chem. 261*, 16155–16160.
Lehrer, S. S., Betteridge, D. R., Graceffa, P., Wong, S., & Seidel, J. C. (1984) *Biochemistry 23*, 1591–1595.
Lowry, O. H., Rosebrough, N. J., Farr, A. L., & Randall, R. J. (1951) *J. Biol. Chem. 193*, 265–275.
Lynch, W. P., Riseman, V. M., & Bretscher, A. (1987) *J. Biol. Chem. 262*, 7429–7437.
Marston, S. B., Lehman, W., Moody, C. J., & Smith, C. W. J. (1985) in *Advances in Protein Phosphatases II* (Merlevede, W., Lens, H., & DiSalvo, J., Eds.) pp 171–189, Leuven University Press, Leuven, Belgium.
Miyata, H., & Chacko, S. (1986) *Biochemistry 25*, 2725–2729.
Ngai, P. K., & Walsh, M. P. (1984) *J. Biol. Chem. 259*, 13656–13659.
Ngai, P. K., & Walsh, M. P. (1985) *Biochem. J. 230*, 695–707.
Smith, C. W. J., Pritchard, K., & Marston, S. B. (1987) *J. Biol. Chem. 262*, 116–122.
Sobue, K., Muramoto, Y., Fujita, M., & Kakiuchi, S. (1981) *Proc. Natl. Acad. Sci. U.S.A. 78*, 5652–5655.
Sobue, K., Morimoto, K., Kanda, K., Maruyama, K., & Kakiuchi, S. (1982) *FEBS Lett. 138*, 289–292.
Sobue, K., Takahashi, K., & Wakabayashi, I. (1985) *Biochem. Biophys. Res. Commun. 132*, 645–651.
Wang, J. L., & Edelman, G. M. (1971) *J. Biol. Chem. 246*, 1185–1191.
Weltman, J. K., Szaro, R. P., Frackelton, A. R., Jr., Dowben, R. M., Binting, J. R., & Cathou, R. E. (1973) *J. Biol. Chem. 248*, 3173.

Gene Sequence and Primary Structure of Mitochondrial Malate Dehydrogenase from *Saccharomyces cerevisiae*[†,‡]

Leslie M. Thompson, Pamela Sutherland, Joan S. Steffan, and Lee McAlister-Henn*

Department of Biological Chemistry, California College of Medicine, University of California, Irvine, California 92717

Received March 24, 1988; Revised Manuscript Received May 26, 1988

ABSTRACT: The nucleotide sequence was determined for a 1.5-kilobase genomic fragment containing the mitochondrial malate dehydrogenase gene (*MDH*1) of *Saccharomyces cerevisiae*. The open-reading frame encodes a precursor form of the mature enzyme containing an amino-terminal extension of 17 amino acid residues. In vitro translation experiments confirm that the initial translation product of *MDH*1 is larger than the mature polypeptide. Transcription of *MDH*1 initiates at several sites from 83 to 97 nucleotides 5′ of the translational start site. Alignment of the amino acid sequence for the mature yeast enzyme with those for mammalian mitochondrial and for *Escherichia coli* malate dehydrogenases reveals polypeptides of very similar sizes with identical amino acids at 54% and 48% of the residue positions, respectively. The amino acid sequences of the yeast and mammalian mitochondrial targeting sequences are similar but less related than the mature polypeptides. The yeast *MDH*1 gene is shown to reside on chromosome XI.

Two forms of malate dehydrogenase, a mitochondrial and a cytoplasmic isozyme, catalyze the NAD^+-dependent oxidation of malate in eucaryotic cells. As components of the malate/aspartate shuttle cycle, this compartmentalized isozyme system represents an important mechanism for exchange of substrates and reducing equivalents between central metabolic pathways separated by the mitochondrial membrane. The mitochondrial and cytoplasmic forms of malate dehydrogenase from many species are dimers of identical subunits with approximate molecular weights of 68 000 and 72 000, respectively (Banaszak & Bradshaw, 1975). X-ray crystallography and amino acid sequence analyses of the porcine isozymes (Birktoft et al., 1982, 1987; Roderick &

[†] Supported by USPHS Research Grant GM 33218.
[‡] The nucleic acid sequence in this paper has been submitted to GenBank under Accession Number J02841.
* To whom correspondence should be addressed.

0006-2960/88/0427-8393$01.50/0